by reaction j producing (consuming) metabolite i by:

$$\dot{x}_{ij} = |S_{ij}|v_j$$

Random uptake conditions

We choose randomly X% (where $X = 10$, 50 or 80) of the 89 potential input substrates that *E. coli* consumes in addition to the minimal uptake basis. For each of the transport reactions, we set the uptake rate to 20 mmol per gram of dry weight per hour. As there are a very large number of possible combinations of the selected input substrates, we repeat this process 5,000 times and average over each realization.

The hit-and-run method

We select a set of basis vectors spanning the solution space using singular-value decomposition. Because the reaction fluxes must be positive, the 'bouncer' is constrained to the part of the solution space that intersects the positive orthant. We constrain the bouncer within a hypersphere of radius R_{max} and outside a hypersphere of radius $R_{min} < R_{max}$ where we find that the sampling results are independent of the choices of R_{min} and R_{max}. Starting from a random initial point inside the positive flux cone in a randomly chosen direction, the bouncer travels deterministically a distance d between sample points. Each sample point, corresponding to a solution vector where the components are the individual fluxes, is normalized by projection onto the unit sphere. After every bth bounce off the internal walls of the flux cone, the direction of the bouncer is randomized.

High-flux backbone

For each metabolite we keep only the reactions with the largest flux that produces and consumes the metabolite. Metabolites that are not produced (consumed) are discounted. Subsequently, a directed link is introduced between two metabolites A and B if (1) A is a substrate of the most active reaction producing B, and (2) B is a product of the maximal reaction consuming A. We consider only metabolites that are connected to at least one other metabolite after steps (1) and (2). For clarity, we remove P_i, PP_i and ADP. Further details and figures are provided in the Supplementary Information.

Received 29 August; accepted 12 December 2003; doi:10.1038/nature02289.

1. Jeong, H., Tombor, B., Albert, R., Oltvai, Z. N. & Barabási, A.-L. The large-scale organization of metabolic networks. *Nature* 407, 651–654 (2000).
2. Wagner, A. & Fell, D. A. The small world inside large metabolic networks. *Proc. R. Soc. Lond. B* 268, 1803–1810 (2001).
3. Ravasz, E., Somera, A. L., Mongru, D. A., Oltvai, Z. N. & Barabási, A.-L. Hierarchical organization of modularity in metabolic networks. *Science* 297, 1551–1555 (2002).
4. Holme, P., Huss, M. & Jeong, H. Subnetwork hierarchies of biochemical pathways. *Bioinformatics* 19, 532–538 (2003).
5. Savageau, M. A. *Biochemical Systems Analysis: a Study of Function and Design in Molecular Biology* (Addison-Wesley, Reading, MA, 1976).
6. Heinrich, R. & Schuster, S. *The Regulation of Cellular Systems* (Chapman & Hall, New York, 1996).
7. Goldbeter, A. *Biochemical Oscillations and Cellular Rhythms: the Molecular Bases of Periodic and Chaotic Behavior* (Cambridge Univ. Press, Cambridge, UK, 1996).
8. Edwards, J. S. & Palsson, B. O. The *Escherichia coli* MG1655 *in silico* metabolic genotype: its definition, characteristics, and capabilities. *Proc. Natl Acad. Sci. USA* 97, 5528–5533 (2000).
9. Edwards, J. S., Ibarra, R. U. & Palsson, B. O. *In silico* predictions of *Escherichia coli* metabolic capabilities are consistent with experimental data. *Nature Biotechnol.* 19, 125–130 (2001).
10. Ibarra, R. U., Edwards, J. S. & Palsson, B. O. *Escherichia coli* K-12 undergoes adaptive evolution to achieve *in silico* predicted optimal growth. *Nature* 420, 186–189 (2002).
11. Edwards, J. S., Ramakrishna, R. & Palsson, B. O. Characterizing the metabolic phenotype: a phenotype phase plane analysis. *Biotechnol. Bioeng.* 77, 27–36 (2002).
12. Segre, D., Vitkup, D. & Church, G. M. Analysis of optimality in natural and perturbed metabolic networks. *Proc. Natl Acad. Sci. USA* 99, 15112–15117 (2002).
13. Blattner, F. R. *et al.* The complete genome sequence of *Escherichia coli* K-12. Science 277, 1453–1474 (1997).
14. Gerdes, S. Y. *et al.* Experimental determination and system level analysis of essential genes in *Escherichia coli* MG1655. *J. Bacteriol.* 185, 5673–5684 (2003).
15. Emmerling, M. *et al.* Metabolic flux responses to pyruvate kinase knockout in *Escherichia coli*. *J. Bacteriol.* 184, 152–164 (2002).
16. Smith, H. L. Efficient Monte-Carlo procedures for generating points uniformly distributed over bounded regions. *Oper. Res.* 32, 1296–1308 (1984).
17. Lovász, L. Hit-and-run mixes fast. *Math. Programm.* 86, 443–461 (1999).
18. Goh, K. I., Kahng, B. & Kim, D. Universal behavior of load distribution in scale-free networks. *Phys. Rev. Lett.* 87, 278701 (2001).
19. Barabási, A.-L. & Albert, R. Emergence of scaling in random networks. *Science* 286, 509–512 (1999).
20. Barthelemy, M., Gondran, B. & Guichard, E. Spatial structure of the Internet traffic. *Physica A* 319, 633–642 (2003).
21. Ma, H. W. & Zeng, A. P. The connectivity structure, giant strong component and centrality of metabolic networks. *Bioinformatics* 19, 1423–1430 (2003).
22. Dandekar, T., Schuster, S., Snel, B., Huynen, M. & Bork, P. Pathway alignment: application to the comparative analysis of glycolytic enzymes. *Biochem. J.* 343, 115–124 (1999).
23. Schuster, S., Fell, D. A. & Dandekar, T. A general definition of metabolic pathways useful for systematic organization and analysis of complex metabolic networks. *Nature Biotechnol.* 18, 326–332 (2000).
24. Stelling, J., Klamt, S., Bettenbrock, K., Schuster, S. & Gilles, E. D. Metabolic network structure determines key aspects of functionality and regulation. *Nature* 420, 190–193 (2002).
25. Sauer, U. *et al.* Metabolic flux ratio analysis of genetic and environmental modulations of *Escherichia coli* central carbon metabolism. *J. Bacteriol.* 181, 6679–6688 (1999).
26. Canonaco, F. *et al.* Metabolic flux response to phosphoglucose isomerase knock-out in *Escherichia coli* and impact of overexpression of the soluble transhydrogenase UdhA. *FEMS Microbiol. Lett.* 204, 247–252 (2001).
27. Fischer, E. & Sauer, U. Metabolic flux profiling of *Escherichia coli* mutants in central carbon metabolism using GC-MS. *Eur. J. Biochem.* 270, 880–891 (2003).
28. Hartwell, L. H., Hopfield, J. J., Leibler, S. & Murray, A. W. From molecular to modular cell biology. *Nature* 402, C47–C52 (1999).
29. Wolf, D. M. & Arkin, A. P. Motifs, modules and games in bacteria. *Curr. Opin. Microbiol.* 6, 125–134 (2003).

Supplementary Information accompanies the paper on **www.nature.com/nature.**

Acknowledgements We thank M. Bárász, J. Becker, E. Ravasz, A. Vazquez and S. Wuchty for discussions; and B. Palsson and S. Schuster for comments on the manuscript. Research at Eötvös University was supported by the Hungarian National Research Grant Foundation (OTKA), and work at the University of Notre Dame and at Northwestern University was supported by the US Department of Energy, the NIH and the NSF.

Competing interests statement The authors declare that they have no competing financial interests.

Correspondence and requests for materials should be addressed to A.-L.B. (alb@nd.edu).

Sortilin is essential for proNGF-induced neuronal cell death

Anders Nykjaer[1,2], Ramee Lee[3], Kenneth K. Teng[3], Pernille Jansen[1,4], Peder Madsen[1], Morten S. Nielsen[1], Christian Jacobsen[1], Marco Kliemannel[5], Elisabeth Schwarz[5], Thomas E. Willnow[2,4], Barbara L. Hempstead[3] & Claus M. Petersen[1]

[1]*Department of Medical Biochemistry, Ole Worms Allé 170, Aarhus University, and* [2]*Receptor Aps, Gustav Wieds vej 10, DK-8000 Aarhus C, Denmark*
[3]*Weill Medical College of Cornell University, New York, New York 10021, USA*
[4]*Max-Delbrück-Center for Molecular Medicine, 13125 Berlin, Germany*
[5]*Institute for Biotechnology, Martin-Luther-Universität, Halle-Wittenberg, 06120 Halle, Germany*

Sortilin[1] (~95 kDa) is a member of the recently discovered family of Vps10p-domain receptors[2,3], and is expressed in a variety of tissues, notably brain, spinal cord and muscle. It acts as a receptor for neurotensin[4,5], but predominates in regions of the nervous system that neither synthesize nor respond to this neuropeptide[6], suggesting that sortilin has additional roles. Sortilin is expressed during embryogenesis[7] in areas where nerve growth factor (NGF) and its precursor, proNGF, have well-characterized effects[6,7]. These neurotrophins can be released by neuronal tissues[8,9], and they regulate neuronal development through cell survival and cell death signalling. NGF regulates cell survival and cell death via binding to two different receptors, TrkA and $p75^{NTR}$ (ref. 10). In contrast, proNGF selectively induces apoptosis through $p75^{NTR}$ but not TrkA[11]. However, not all $p75^{NTR}$-expressing cells respond to proNGF, suggesting that additional membrane proteins are required for the induction of cell death. Here we report that proNGF creates a signalling complex by simultaneously binding to $p75^{NTR}$ and sortilin. Thus sortilin acts as a co-receptor and molecular switch governing the $p75^{NTR}$-mediated pro-apoptotic signal induced by proNGF.

Binding of NGF was examined by surface-plasmon resonance (SPR). As demonstrated in Fig. 1a, sortilin bound mature NGF with moderate affinity (dissociation constant (K_d) ~90 nM). In contrast, the affinity of NGF for $p75^{NTR}$ and TrkA was high (K_d 1–2 nM), in accordance with previous studies in cells[11–13]. As the NGF precursor (proNGF) may escape intracellular processing and be released extracellularly, we next examined binding of proNGF[9,11,14,15]. Whereas lack of processing reduces the affinity of proNGF for $p75^{NTR}$ and TrkA (K_d ~15–20 nM), it results in a much higher affinity (K_d ~5 nM) for sortilin (Fig. 1a). This is surprising because

proNGF has been reported to interact with cellular $p75^{NTR}$, but not TrkA, with a higher affinity (K_d ~0.2 nM) than mature NGF, and to selectively induce $p75^{NTR}$-dependent apoptosis in neurons, smooth muscle cells and oligodendrocytes[8,11]. Our data may reflect the participation of a $p75^{NTR}$ co-receptor, and this receptor might be sortilin (see below).

To examine the structural basis of proNGF binding, we produced the pro domain of proNGF as a glutathione *S*-transferase fusion protein (GST–pro) (Fig. 1b). The GST–pro protein bound to sortilin with an affinity very similar to that of proNGF (K_d ~8 nM), but not to $p75^{NTR}$ or TrkA (Fig. 1a). Additional experiments further demonstrated that binding of proNGF to sortilin was inhibited markedly (>75%) by neurotensin, and was almost abolished in the presence of GST–pro (Fig. 1c). Thus, the pro domain constitutes the structural basis for the high-affinity binding between proNGF and sortilin.

We next assessed binding of proNGF to cellular sortilin. We transfected 293 cells without endogenous sortilin with the receptor constructs indicated in Fig. 2a, and evaluated binding of proNGF at 37 °C. Control cells demonstrated no binding or uptake of ligand, whereas cells expressing wild-type sortilin exhibited significant endocytosis of proNGF (Fig. 2b), but not of mature NGF (Fig. 2c). The observed uptake was hampered strongly in the presence of excess neurotensin or GST–pro (data not shown). Furthermore, transfectants expressing a mutant sortilin protein (sortilin(mut)) that accumulates on the plasma membrane owing to disrupted motifs for endocytosis[16], displayed intense surface labelling with proNGF, but little uptake.

Binding and uptake of proNGF was also investigated in cells transfected with TrkA and $p75^{NTR}$, and in cells expressing each of the two receptors in combination with sortilin (Fig. 2b). TrkA transfectants exhibited a very modest uptake of proNGF, and on co-transfection with sortilin, endocytosis of proNGF was comparable to that observed in cells expressing sortilin alone. In contrast, uptake of mature NGF was efficient in TrkA-expressing cells and was unaffected by co-transfection with sortilin (Fig. 2c). In $p75^{NTR}$ transfectants, proNGF as well as mature NGF was almost exclusively found on the plasma membrane, indicating a slow or insignificant endocytosis (Fig. 2b, c) consistent with prior observations[17,18]. However, coexpression of $p75^{NTR}$ with sortilin re-established uptake of proNGF, and coexpression with sortilin(mut), as well as with wild-type sortilin, induced a significant increase in surface-associated ligand, suggesting a synergistic rather than a simple additive effect of sortilin and $p75^{NTR}$ coexpression.

The findings demonstrate that sortilin exhibits negligible binding of NGF, but also that it conveys a significantly higher capacity for uptake of proNGF than either of the two established receptors (that is, $p75^{NTR}$ and TrkA). Moreover, results in double transfectants suggest that sortilin and $p75^{NTR}$ cooperate to promote proNGF binding.

To characterize the molecular mechanisms underlying the putative cooperativity between $p75^{NTR}$ and sortilin, affinity crosslinking was performed. Crosslinking of ^{125}I-labelled proNGF to $p75^{NTR}$ and sortilin double transfectants produced labelled complexes of ~110, ~140 and ~240 kDa (Fig. 3a, lane 1), but was unproductive in single transfectants, suggesting that coexpression of sortilin and $p75^{NTR}$ is required for efficient binding at subnanomolar concentrations of proNGF (Fig. 3a, lanes 5–6). Furthermore, immunoprecipitation with receptor antisera established that both sortilin and $p75^{NTR}$ were components of the crosslinked adducts (Fig. 3a, lanes 7–8). Similar experiments performed on cells coexpressing $p75^{NTR}$ and sortilin(mut), which has a higher surface expression than wild-type sortilin[16], resulted in a quantitative increase in crosslinked complexes (data not shown). Finally, generation of the crosslinking adducts was markedly reduced in the presence of unlabelled proNGF, neurotensin or GST–pro, implying that sortilin, as well as the NGF pro domain, is critical to complex formation (Fig. 3a, lanes 2–4).

We conclude that the ~240 kDa adduct probably represents a heterotrimeric complex comprising proNGF, sortilin and $p75^{NTR}$, whereas the ~110 kDa and ~140 kDa species constitute proNGF in association with a single receptor. Expression of both receptors is required for efficient binding of proNGF, and our results support a model in which the pro domain and the 'mature' part of proNGF simultaneously engage sortilin and $p75^{NTR}$, respectively.

Corresponding experiments established that proNGF does not form stable complexes with TrkA (Fig. 3b). In fact, crosslinking with proNGF using cells expressing all three receptors (TrkA, $p75^{NTR}$ and sortilin) resulted in ~110, ~140 and ~240 kDa adducts that could be precipitated with anti-sortilin (data not shown) and anti-$p75^{NTR}$ antibodies but not with TrkA-specific antiserum. Thus, proNGF discriminates between TrkA and $p75^{NTR}$ in cells that express both receptors in combination with sortilin.

In accordance with previous reports[12,13], crosslinking using mature ^{125}I-labelled NGF yielded complexes with both $p75^{NTR}$ (~90 and ~180 kDa) and TrkA (~160 kDa) (Fig. 3c). However,

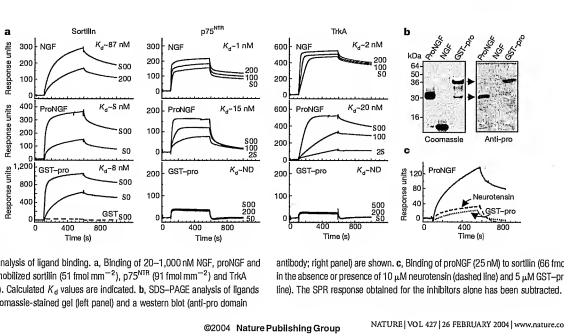

Figure 1 SPR analysis of ligand binding. **a**, Binding of 20–1,000 nM NGF, proNGF and GST–pro to immobilized sortilin (51 fmol mm^{-2}), $p75^{NTR}$ (91 fmol mm^{-2}) and TrkA (66 fmol mm^{-2}). Calculated K_d values are indicated. **b**, SDS–PAGE analysis of ligands used in **a**. A Coomassie-stained gel (left panel) and a western blot (anti-pro domain antibody; right panel) are shown. **c**, Binding of proNGF (25 nM) to sortilin (66 fmol mm^{-2}) in the absence or presence of 10 μM neurotensin (dashed line) and 5 μM GST–pro (dotted line). The SPR response obtained for the inhibitors alone has been subtracted.

no additional crosslinked complexes were observed when either of the two was coexpressed with sortilin, and sortilin single transfectants did not bind NGF. These results indicate that sortilin neither interacts with mature NGF nor is part of a complex formed on binding of mature NGF to $p75^{NTR}$ or TrkA.

We next examined whether sortilin and $p75^{NTR}$ physically associate on the cell membrane. Cells expressing both receptors were biolabelled and incubated in the absence or presence of proNGF, followed by treatment with a membrane-impermeable reducible crosslinker, lysis and immunoprecipitation using anti-$p75^{NTR}$ antibodies. Sortilin could be crosslinked directly to $p75^{NTR}$ (Fig. 3d). However, in the presence of proNGF, the relative amount of crosslinked and co-precipitated sortilin increased by about fivefold (3.9% to 18.4%). Equilibrium binding studies were then designed to determine whether $p75^{NTR}$ and sortilin coexpression might influence the specificity and affinity of ligand binding. As demonstrated in Fig. 3e, ^{125}I-labelled NGF bound to cells coexpressing sortilin and $p75^{NTR}$ with an estimated K_d of ~1.0 nM. This agrees with previous results[12] obtained in $p75^{NTR}$-expressing cells, and as sortilin single transfectants did not bind mature NGF (data not shown), the data indicate that mature NGF binds strictly to $p75^{NTR}$. In contrast, similar experiments with ^{125}I-labelled proNGF further indicated that sortilin and $p75^{NTR}$ cooperate in proNGF binding. Thus, cells expressing a single receptor type—either sortilin or $p75^{NTR}$—did not bind ^{125}I-labelled proNGF (data not shown), whereas cells coexpressing these receptors did. Scatchard analysis (Fig. 3e) suggested fewer binding sites for proNGF than for NGF in the double transfectants, but also a higher affinity for proNGF (K_d ~160 pM) that could not be accounted for by binding to any single receptor. Accordingly, A875 cells, which bind proNGF with high affinity[11], express high levels of endogenous sortilin and $p75^{NTR}$

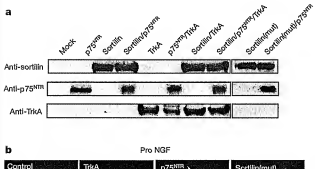

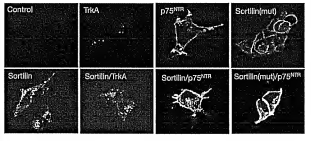

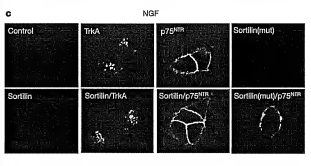

Figure 2 Binding and uptake of proNGF and NGF in 293 cells. **a**, Western blot showing the level of receptor expression in the transfected 293 cells. **b**, **c**, Untransfected cells (control) and cells transfected with the indicated receptors were incubated (37 °C, 45 min) with 50 nM proNGF (**b**) or NGF (**c**) before fixation and staining with anti-NGF antibodies.

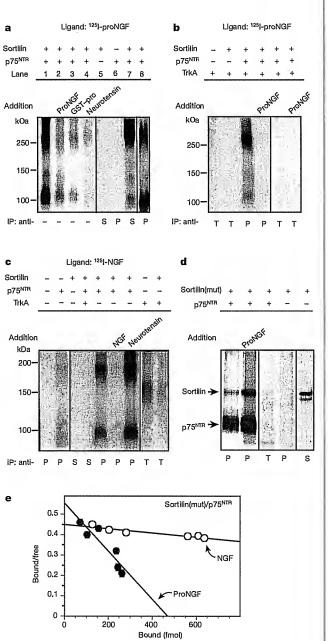

Figure 3 ProNGF-induced formation of heterotrimeric complexes comprising sortilin and $p75^{NTR}$. **a**–**c**, Crosslinking of ^{125}I-labelled proNGF (**a**, **b**) or ^{125}I-labelled NGF (**c**) to transfected 293 cells in the presence and absence of excess proNGF, NGF, GST–pro or neurotensin. Cell lysates (—) and immunoprecipitated proteins were subjected to SDS–PAGE and labelled bands were visualized by autoradiography. Antibodies used for immunoprecipitation (IP) of sortilin (S), $p75^{NTR}$ (P) and TrkA (T) are indicated. **d**, Biolabelled cells overexpressing sortilin(mut) and $p75^{NTR}$ were incubated with and without proNGF (25 nM) and treated with a reducible crosslinker. Autoradiographic bands resulting from reducing SDS–PAGE of immunoprecipitates are shown. **e**, Scatchard plot showing binding of radiolabelled NGF (open circles) and proNGF (closed circles) to cells expressing sortilin(mut) and $p75^{NTR}$.

(Fig. 4a). The results support a model in which proNGF binds to and promotes the formation of a multi-component receptor complex comprising both sortilin and $p75^{NTR}$.

ProNGF is more efficient than NGF in inducing apoptosis in superior cervical ganglion (SCG) neurons, vascular smooth muscle (SM-11) cells and oligodendrocytes, and in promoting chemotaxis and ligand binding in A875 melanoma cells[9,11,19]. These cell types all express significant levels of sortilin and $p75^{NTR}$ (Fig. 4a). We found that uptake of proNGF in dissociated SCG cultures was inhibited by the GST–pro protein (data not shown), which selectively inhibits binding to sortilin. Moreover, crosslinking of ^{125}I-labelled proNGF to SM-11 cells resulted in labelled adducts of ~110, ~140 and ~240 kDa, similar to those obtained in the $p75^{NTR}$ and sortilin double transfectants (Fig. 4b). These findings suggest that the biological effects of proNGF require coexpression of sortilin and $p75^{NTR}$. To assess directly whether binding of proNGF to sortilin regulates biological action, the ability of GST–pro and neurotensin to impair proNGF actions was evaluated. In order to minimize conversion of proNGF into mature NGF, which might introduce a bias by facilitating survival in TrkA-positive cells, a furin-resistant mutant of proNGF[11] was used in all subsequent experiments, unless otherwise stated. In SM-11 cells co-expressing $p75^{NTR}$ and sortilin, furin-resistant proNGF was more effective than mature NGF in inducing cell death as assessed by a TdT-mediated dUTP nick end labelling (TUNEL) assay (Fig. 4c). In addition, wild-type proNGF induced apoptosis as effectively as furin-resistant proNGF (data not shown). Co-incubation of proNGF with an excess of neurotensin, or with excess GST–pro, but not GST alone, impaired the induction of cell death and apoptosis by more than 90% (Fig. 4c). Similar findings were obtained in cultured SCG neurons expressing sortilin and $p75^{NTR}$ as well as TrkA. Thus, both GST–pro and neurotensin significantly reduced proNGF-induced apoptosis in SCG neurons,

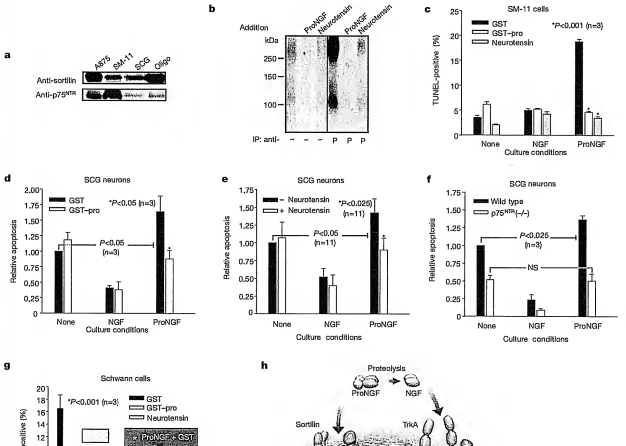

Figure 4 Sortilin is required for the pro-apoptotic action of proNGF. **a**, Receptor expression in proNGF-responsive cell types. **b**, Crosslinking of ^{125}I-labelled proNGF to SM-11 cells and inhibition by unlabelled competitors. **c–e**, ProNGF-induced apoptosis (cell type indicated) and its inhibition by GST, GST–pro and neurotensin. The number of apoptotic and total cells counted per condition was 100/~300 (**d** and **f**) and 300/~1,100 (**e**). All values are normalized to apoptosis in the absence of any additions. **f**, Killing of SCG neurons from wild-type and $p75^{NTR}$ knockout mice. **g**, ProNGF-induced apoptosis of Schwann cells transiently transfected with sortilin. Columns indicate per cent of TUNEL-positive cells among cells that express (S+) or lack (S–) sortilin. Left inset shows western blot of Schwann cell lysate; right inset shows apoptotic nuclei (TUNEL-positive, green) in transfectants expressing sortilin (red staining). Asterisk indicates an untransfected cell. **h**, Schematic model of receptor–complex formation.

whereas neither affected neuronal survival in response to mature NGF or on NGF withdrawal (Fig. 4d, e). As shown in Fig. 4f, $p75^{NTR}$-deficient neurons from $p75^{NTR}$ knockout mice[20] that express sortilin in the absence of $p75^{NTR}$ (data not shown) exhibit NGF-dependent survival, but are resistant to proNGF-induced killing. A similar resistance to proNGF was seen in Schwann cells expressing $p75^{NTR}$ but not sortilin (Fig. 4g); however, after transfection with sortilin, Schwann cells became sensitive to proNGF-induced apoptosis. Approximately 95% of the cells that expressed sortilin (~18% of total) were TUNEL positive, and among all TUNEL-positive cells ~96% expressed both sortilin and $p75^{NTR}$. This sensitivity to proNGF-induced killing was reversed by co-incubation with GST–pro (Fig. 4g) and neurotensin, which blocked binding of proNGF to sortilin. It follows that both receptors are obligate for the induction of proNGF-mediated cell death, whereas sortilin expression has no impact on NGF responsiveness under these circumstances.

We conclude that proNGF targets and promotes formation of a signalling complex comprising endogenous sortilin and $p75^{NTR}$, and that both receptors are required for proNGF-mediated apoptosis. In contrast, mature NGF preferentially binds $p75^{NTR}$ and/or TrkA, with sortilin having little or no bearing on NGF-initiated signalling.

Our study indicates that the neurotrophins use not two but three distinct receptor classes to dictate and regulate opposing biological responses of survival and death. We identify sortilin as a biologically important neurotrophin receptor that targets the pro domain of proNGF with high affinity. The present data suggest that sortilin is a required component for transmitting proNGF-dependent death signals via $p75^{NTR}$. Together with $p75^{NTR}$, sortilin facilitates the formation of a composite high-affinity binding site for proNGF (Fig. 4h). Thus, sortilin serves as a co-receptor and molecular switch, enabling neurons expressing Trk and $p75^{NTR}$ to respond to a pro-neurotrophin and to initiate pro-apoptotic rather than pro-survival actions. In the absence of sortilin, regulated activity of extracellular proteases may cleave proNGF to mature NGF[11], promoting Trk-mediated survival signals (Fig. 4h). In conclusion, NGF-induced neuronal survival and death is far more complicated than previously appreciated, as it depends on an intricate balance between proNGF and mature NGF, as well as on the spatial and temporal expression of three distinct receptors: TrkA, $p75^{NTR}$ and sortilin. As sortilin is but one member of the Vps10p-domain receptor family expressed in the nervous system, future studies should show whether other pro-neurotrophins use related Vps10p-containing receptors to switch biological responsivity to neurotrophin isoforms. □

Methods

Recombinant proteins and radiolabelling

Human proNGF and mature NGF generated in *Escherichia coli*[21] were a gift from Scil Proteins GmbH. Radioiodinated ligands[8,22] (~3,000 d.p.m. $fmol^{-1}$) were used within 48 h of iodination and their integrity and bioactivity was assayed by SDS–polyacrylamide gel electrophoresis (PAGE), PC12 cell neuritogenesis (NGF) and apoptosis of $p75^{NTR}$-expressing vascular smooth muscle cells (proNGF). Mature NGF and furin-resistant mouse proNGF were purified from media of transfected 293 cells[11]. The NGF pro domain (amino acids E19 to R121) was expressed in *E. coli* as a GST fusion protein and purified on glutathione–agarose beads. The luminal domain of sortilin was expressed and purified as described[4]. $p75^{NTR}$-Fc and TrkA-Fc (fusion proteins) were from R&D Systems.

SPR analysis, equilibrium binding and western blotting

The SPR analysis was performed essentially as described[8,24]. The receptors were immobilized (at 10–15 μg ml^{-1}) on a CM5 chip and remaining coupling sites were blocked with 1 M ethanolamine. Sample and running buffer was 10 mM HEPES, 150 mM $(NH_4)_2SO_4$, 1.5 mM $CaCl_2$, 1 mM EGTA, 0.005% Tween-20 pH 7.4. After each analytic cycle the sensor chip was regenerated in a 10 mM glycine-HCl buffer. The SPR signal was expressed in relative response units (RU); that is, the response obtained in a control flow channel was subtracted. Kinetic parameters were determined using BIAevaluation 3.1 software. Equilibrium-binding studies were performed as described[8]. In brief, the cells (2×10^6 ml^{-1}) were incubated (4 °C, 40 min) with radioiodonated NGF or proNGF ($2–20 \times 10^{-10}$ M) in the presence or absence of a 500-fold molar excess of NGF or neurotensin, respectively. Bound ligand was then separated from free ligand by centrifugation through calf serum. Mean values of triplicates (from two independent experiments) were evaluated using the PRISM program.

Western blotting, after reducing SDS–PAGE, was performed using a rabbit antibody (1:1,000) directed against the pro domain of NGF (amino acids 23–81) of human NGF[8] and horseradish-peroxidase-conjugated swine anti-rabbit immunoglobulin (Amersham Biosciences).

Transfected cell lines

Parental 293 cells and transfectants expressing $p75^{NTR}$ or $TrkA^{11}$ were transfected with wild-type sortilin[4] or the sortilin(mut) variant impaired in endocytosis (alanine substituted for Y14, L17, L51 and L52 in the cytoplasmic tail)[24], and selected using zeocin. Primary rat Schwann cells[25], plated on polylysine-coated plates, were transfected with pcDNA wild-type sortilin[4] or pcDNA alone using calcium phosphate.

Crosslinking, biolabelling and immunoprecipitation

Cells (2×10^6 ml^{-1}) were incubated (4 °C, 2 h) with radioiodinated proNGF or NGF (400 pM), in the absence or presence of 100 nM unlabelled proNGF, 40 μM neurotensin or 200 nM GST or GST–pro, followed by crosslinking (15 min) with 4 mM 1-ethyl-3-[3-dimethylaminopropyl]carbodiimide and 25 mM DSS (Pierce). Washed cells were subsequently lysed in 1% Nonidet P40 buffer containing protease inhibitors and precipitations were performed using anti-$p75^{NTR}$ and anti-TrkA antisera[13], and anti-sortilin antibody[4].

Transfected cells were biolabelled (3–4 h) with L-[^{35}S]cysteine and L-[^{35}S]methionine, then incubated (20 °C, 2 h) with or without 25 nM proNGF and, finally, treated (30 min) with 5 mM of the reducible crosslinker DTSSP (Pierce) before lysis in 1% Triton-X100 buffer containing protease inhibitors[4,26]. Immunoprecipitation was performed using rabbit anti-$p75^{NTR}$ (number 9993), anti-Trk (Santa Cruz) and anti-sortilin[4]. All precipitated proteins were analysed by reducing SDS–PAGE and were detected by autoradiography.

Induction of apoptosis in various cells

A vascular smooth muscle cell line expressing human $p75^{NTR}$ but not $TrkA^{27}$ was incubated (16 h) with 2 ng ml^{-1} of mature NGF or furin-resistant proNGF[11] in the presence of 50 nM GST or GST–pro, or 40 μM neurotensin. After fixation, cells were fixed, incubated with 4,6-diamidino-2-phenylindole (DAPI) and subjected to TUNEL analysis (Roche Molecular Biochemicals). Results represent the mean value of three independent experiments performed in triplicate. At least 300 cells per condition were counted.

Dissociated P0–P1 rat SCG neurons[28] or mouse SCG neurons obtained from $p75^{-NTR}$ knockout mice[20] or wild-type littermates were plated on collagen-coated slides and maintained for 5 days in 50 ng ml^{-1} NGF before use. Replicate cultures were rinsed five times with NGF-free medium and treated with or without the given additives, as indicated. After 36 h SCG cultures were processed for TUNEL analysis and counterstained with anti-neuronal-specific β-tubulin (Tuj1, Covance)[11]. TUNEL-positive neurons were scored blindly by the observer and at least 100 cells were counted for each culture condition.

Transfected Schwann cells were plated on 8-well slides (NUNC) at 20,000 cells per well. At 48 h after transfection, cells were treated (18 h) with 5 ng ml^{-1} mature NGF, purified recombinant cleavage-resistant proNGF or diluent alone. After fixation, the cells were stained using mouse anti-sortilin antibody (Transduction Biolabs, anti-NTR3 612101) and rhodamine goat anti-mouse IgG followed by DAPI incubation, and then subjected to TUNEL analysis (Roche Molecular Biochemicals). At least 1,000 cells per condition were counted in a blinded manner, and results are representative of three independent experiments. Where appropriate, statistical significance was determined by Student's *t*-test.

Received 3 November; accepted 23 December 2003; doi:10.1038/nature02319.

1. Petersen, C. M. *et al.* Molecular identification of a novel candidate sorting receptor purified from human brain by receptor-associated protein affinity chromatography. *J. Biol. Chem.* **272,** 3599–3605 (1997).
2. Hermey, G. *et al.* Characterization of sorCS1, an alternatively spliced receptor with completely different cytoplasmic domains that mediate different trafficking in cells. *J. Biol. Chem.* **278,** 7390–7396 (2003).
3. Jacobsen, L. *et al.* Activation and functional characterization of the mosaic receptor SorLA/LR11. *J. Biol. Chem.* **276,** 22788–22796 (2001).
4. Mazella, J. *et al.* The 100-kDa neurotensin receptor is gp95/sortilin, a non-G-protein-coupled receptor. *J. Biol. Chem.* **273,** 26273–26276 (1998).
5. Munck, P. C. *et al.* Propeptide cleavage conditions sortilin/neurotensin receptor-3 for ligand binding. *EMBO J.* **18,** 595–604 (1999).
6. Sarret, P. *et al.* Distribution of NTS3 receptor/sortilin mRNA and protein in the rat central nervous system. *J. Comp. Neurol.* **461,** 483–505 (2003).
7. Hermans-Borgmeyer, I., Hermey, G., Nykjaer, A. & Schaller, C. Expression of the 100-kDa neurotensin receptor sortilin during mouse embryonal development. *Brain Res. Mol. Brain Res.* **65,** 216–219 (1999).
8. Beattie, M. S. *et al.* ProNGF induces p75-mediated death of oligodendrocytes following spinal cord injury. *Neuron* **36,** 375–386 (2002).
9. Hazan, W., Pedchenko, T., Krtzsan-Agbas, D., Bourn, L. & Smith, P. G. Sympathetic neurons synthesize and secrete pro-nerve growth factor protein. *J. Neurobiol.* **57,** 38–53 (2003).
10. Chao, M. V. Neurotrophins and their receptors: a convergence point for many signalling pathways. *Nature Rev. Neurosci.* **4,** 299–309 (2003).
11. Lee, R., Kermani, P., Teng, K. K. & Hempstead, B. L. Regulation of cell survival by secreted proneurotrophins. *Science* **294,** 1945–1948 (2001).
12. Esposito, D. *et al.* The cytoplasmic and transmembrane domains of the p75 and Trk A receptors regulate high affinity binding to nerve growth factor. *J. Biol. Chem.* **276,** 32687–32695 (2001).

13. Mahadeo, D., Kaplan, L., Chao, M. V. & Hempstead, B. L. High affinity nerve growth factor binding displays a faster rate of association than p140trk binding. Implications for multi-subunit polypeptide receptors. *J. Biol. Chem.* 269, 6884–6891 (1994).
14. Fahnestock, M., Michalski, B., Xu, B. & Coughlin, M. D. The precursor pro-nerve growth factor is the predominant form of nerve growth factor in brain and is increased in Alzheimer's disease. *Mol. Cell Neurosci.* 18, 210–220 (2001).
15. Heymach, J. V. Jr & Shooter, E. M. The biosynthesis of neurotrophin heterodimers by transfected mammalian cells. *J. Biol. Chem.* 270, 12297–12304 (1995).
16. Nielsen, M. S. *et al.* The sortilin cytoplasmic tail conveys Golgi-endosome transport and binds the VHS domain of the GGA2 sorting protein. *EMBO J.* 20, 2180–2190 (2001).
17. Gregano, N., Levi, A. & Alema, S. Modulation of nerve growth factor internalization by direct interaction between p75 and TrkA receptors. *J. Neurosci. Res.* 50, 1–12 (1997).
18. Bronfman, F. C., Tcherpakov, M., Jovin, T. M. & Fainzilber, M. Ligand-induced internalization of the p75 neurotrophin receptor: a slow route to the signaling endosome. *J. Neurosci.* 23, 3209–3220 (2003).
19. Shonukan, O., Bagayogo, I., McCrea, P., Chao, M. & Hempstead, B. Neurotrophin-induced melanoma cell migration is mediated through the actin-bundling protein fascin. *Oncogene* 22, 3616–3623 (2003).
20. Lee, K. F. *et al.* Targeted mutation of the gene encoding the low affinity NGF receptor p75 leads to deficits in the peripheral sensory nervous system. *Cell* 69, 737–749 (1992).
21. Rottenhoff, A. *et al.* The pro-sequence facilitates folding of human nerve growth factor from *Escherichia coli* inclusion bodies. *Eur. J. Biochem.* 268, 3296–3303 (2001).
22. Hempstead, B. L., Schleifer, L. S. & Chao, M. V. Expression of functional nerve growth factor receptors after gene transfer. *Science* 243, 373–375 (1989).
23. Hempstead, B. L., Martin-Zanca, D., Kaplan, D. R., Parada, L. F. & Chao, M. V. High-affinity NGF binding requires coexpression of the trk proto-oncogene and the low-affinity NGF receptor. *Nature* 350, 678–683 (1991).
24. Nykjaer, A. *et al.* Cubilin dysfunction causes abnormal metabolism of the steroid hormone 25(OH) vitamin D(3). *Proc. Natl Acad. Sci. USA* 98, 13895–13900 (2001).
25. Einheber, S., Milner, T. A., Giancotti, F. & Salzer, J. L. Axonal regulation of Schwann cell integrin expression suggests a role for $\alpha 6\beta 4$ in myelination. *J. Cell Biol.* 123, 1223–1236 (1993).
26. Nykjaer, A. *et al.* Mannose 6-phosphate/insulin-like growth factor-II receptor targets the urokinase receptor to lysosomes via a novel binding interaction. *J. Cell Biol.* 141, 815–828 (1998).
27. Wang, S. *et al.* p75(NTR) mediates neurotrophin-induced apoptosis of vascular smooth muscle cells. *Am. J. Pathol.* 157, 1247–1258 (2000).
28. Mitsui, C., Sakai, K., Ninomiya, T. & Koike, T. Involvement of TLCK-sensitive serine protease in colchicine-induced cell death of sympathetic neurons in culture. *J. Neurosci. Res.* 66, 601–611 (2001).
29. Bamji, S. X. *et al.* The p75 neurotrophin receptor mediates neuronal apoptosis and is essential for naturally occurring sympathetic neuron death. *J. Cell Biol.* 140, 911–923 (1998).

Acknowledgements We thank M. V. Chao and G. R. Lewin for valuable discussions. J. Salzer, R. Kraemer and P. Fischer are acknowledged for reagents and advice, and S. Tevar for assistance in $p75^{NTR}$ mice genotyping. This work was supported by the Novo Nordisk Foundation, The Danish Medical Research Council, The Carlsberg Foundation (A.N. and C.M.P.) and the NIH (B.L.H. and R.L.).

Competing interests statement The authors declare that they have no competing financial interests.

Correspondence and requests for materials should be addressed to A.N. (an@biokemi.au.dk).

The cytoplasmic body component TRIM5α restricts HIV-1 infection in Old World monkeys

Matthew Stremlau[1], Christopher M. Owens[1], Michel J. Perron[1], Michael Kiessling[1], Patrick Autissier[2] & Joseph Sodroski[1,3]

[1]*Department of Cancer Immunology and AIDS, Dana-Farber Cancer Institute, Department of Pathology, Division of AIDS, and* [2]*Division of Viral Pathogenesis, Beth Israel Deaconess Medical Center, Department of Medicine, Division of AIDS, Harvard Medical School, Boston, Massachusetts 02115, USA*
[3]*Department of Immunology and Infectious Diseases, Harvard School of Public Health, Boston, Massachusetts 02115, USA*

Host cell barriers to the early phase of immunodeficiency virus replication explain the current distribution of these viruses among human and non-human primate species[1–4]. Human immunodeficiency virus type 1 (HIV-1), the cause of acquired immunodeficiency syndrome (AIDS) in humans, efficiently enters the cells of Old World monkeys but encounters a block before reverse transcription[5–4]. This species-specific restriction acts on the incoming HIV-1 capsid[5–7] and is mediated by a dominant reverse factor[7–9]. Here we identify TRIM5α, a component of cytoplasmic bodies, as the blocking factor. HIV-1 infection is restricted more efficiently by rhesus monkey TRIM5α than by human TRIM5α. The simian immunodeficiency virus, which naturally infects Old World monkeys[10], is less susceptible to the TRIM5α-mediated block than is HIV-1, and this difference in susceptibility is due to the viral capsid. The early block to HIV-1 infection in monkey cells is relieved by interference with TRIM5α expression. Our studies identify TRIM5α as a species-specific mediator of innate cellular resistance to HIV-1 and reveal host cell components that modulate the uncoating of a retroviral capsid.

Recombinant HIV-1 expressing green fluorescent protein and pseudotyped with the vesicular stomatitis virus (VSV) G glycoprotein (denoted HIV-1–GFP) can efficiently infect the cells of many mammalian species including humans, but not those of Old World monkeys[5–9]. Here we used a murine leukaemia virus vector to transduce human HeLa cells, which are susceptible to HIV-1–GFP infection, with a complementary DNA library prepared from primary rhesus monkey lung fibroblasts (PRL cells). Two independent HeLa clones resistant to HIV-1–GFP infection, but susceptible to infection with recombinant simian immunodeficiency virus (SIV–GFP) or murine leukaemia virus (MLV–GFP), were identified in a screen (Methods).

The only monkey cDNA insert common to both HIV-1–GFP-resistant clones was predicted to encode TRIM5α, a member of the tripartite motif (TRIM) family of proteins containing RING domains, B-boxes and coiled coils[11–13]. TRIM5α also contains a carboxy-terminal B30.2 (SPRY) domain not found in the other TRIM5 isoforms (ref. 13 and Fig. 1a). The natural functions of TRIM5α, or of the cytoplasmic bodies in which the TRIM5 proteins localize[13,14], are unknown. One TRIM5 isoform has been shown to have ubiquitin ligase activity typical of RING-containing proteins[14]. TRIM5 proteins are expressed constitutively in many tissues[13], consistent with the pattern of expression expected for the HIV-1-blocking factor in monkeys[4].

HeLa cells stably expressing rhesus monkey TRIM5α ($TRIM5\alpha_{rh}$) and control HeLa cells containing empty vector were incubated with different amounts of recombinant HIV-1–GFP, SIV–GFP and MLV–GFP. Expression of $TRIM5\alpha_{rh}$ resulted in a marked inhibition of infection by HIV-1–GFP, whereas MLV–GFP infected control and $TRIM5\alpha_{rh}$-expressing HeLa cells equivalently (Fig. 1b, c). $TRIM5\alpha_{rh}$ inhibited infection by SIV–GFP less efficiently than that by HIV-1–GFP (Fig. 1c). Stable $TRIM5\alpha_{rh}$ expression also inhibited the replication of infectious HIV-1 in HeLa-CD4 cells, which express the receptors for HIV-1 (ref. 15 and Fig. 1d). The replication of a simian–human immunodeficiency virus (SHIV) chimaera, which contains core proteins (including the capsid protein) of SIV_{mac} (ref. 16), was not inhibited in these $TRIM5\alpha_{rh}$-expressing cells. When the infections were done with eightfold more HIV-1 and SHIV, similar results were obtained (Supplementary Information). We conclude that expression of $TRIM5\alpha_{rh}$ specifically and efficiently blocks infection by HIV-1, and exerts a slight inhibitory effect on infection by SIV_{mac}.

To investigate the viral target of the $TRIM5\alpha_{rh}$-mediated restriction, HeLa cells expressing $TRIM5\alpha_{rh}$ or control HeLa cells were incubated with recombinant HIV-1–GFP, SIV–GFP, SIV(HCA-p2)–GFP or HIV(SCA)–GFP. SIV(HCA-p2)–GFP is identical to SIV–GFP, except that the SIV capsid and adjacent p2 sequences have been replaced by those of HIV-1 (ref. 17), and SIV(HCA-p2)–GFP has been shown to be susceptible to the block in Old World monkey cells[5,7]. HIV(SCA)–GFP is identical to HIV-1–GFP, except that most of the capsid protein has been replaced by that of SIV[8], and HIV(SCA)–GFP has been shown to be less susceptible than HIV-1 to the block in Old World monkey cells[9]. We found that HIV-1–GFP and SIV(HCA-p2)–GFP infections were restricted to the same extent in $TRIM5\alpha_{rh}$-expressing HeLa cells, whereas infec-